

# A spectroscopic study of IRAS F10214+4724

Stephen Serjeant<sup>1,2</sup>, Steve Rawlings<sup>2</sup>, Mark Lacy<sup>2</sup>, Richard G. McMahon<sup>3</sup>,  
Andy Lawrence<sup>4</sup>, Michael Rowan-Robinson<sup>1</sup>, Matt Mountain<sup>5</sup>

<sup>1</sup> *Astrophysics Group, Imperial College London, Blackett Laboratory, Prince Consort Road, London SW7 2BZ*

<sup>2</sup> *Astrophysics, Department of Physics, Keble Road, Oxford, OX1 3RH*

<sup>3</sup> *Institute of Astronomy, The Observatories, Madingley Road, Cambridge, CB3 0HA*

<sup>4</sup> *Institute for Astronomy, University of Edinburgh, Royal Observatory, Blackford Hill, Edinburgh EH9 3HJ*

<sup>5</sup> *Gemini 8-M Telescopes Project, 950 N. Cherry Avenue, Tucson, Arizona, 85726, USA*

5 April 2021

## ABSTRACT

The  $z = 2.286$  IRAS galaxy F10214+4724 remains one of the most luminous galaxies in the Universe, despite its gravitational lens magnification. We present optical and near-infrared spectra of F10214+4724, with clear evidence for three distinct components: lines of width  $\sim 1000 \text{ km s}^{-1}$  from a Seyfert-II nucleus;  $\lesssim 200 \text{ km s}^{-1}$  lines which are likely to be associated with star formation; and a broad ( $\sim 4000 \text{ km s}^{-1}$ ) CIII] 1909Å emission line which is blue-shifted by  $\sim 1000 \text{ km s}^{-1}$  with respect to the Seyfert-II lines. Our study of the Seyfert-II component leads to several new results, including: (i) From the double-peaked structure in the Ly $\alpha$  line, and the lack of Ly $\beta$ , we argue that the Ly $\alpha$  photons have emerged through a neutral column of  $N_{\text{H}} \sim 2.5 \times 10^{25} \text{ m}^{-2}$ , possibly located within the AGN narrow-line region as argued in several high redshift radiogalaxies. (ii) The resonant OVI 1032, 1036Å doublet (previously identified as Ly $\beta$ ) is in an optically thick (1:1) ratio. At face value this implies an extreme density ( $n_e \sim 10^{17} \text{ m}^{-3}$ ) more typical of broad line region clouds. However, we attribute this instead to the damping wings of Ly $\beta$  from the resonant absorption. (iii) A tentative detection of HeII 1086 suggests little extinction in the rest-frame ultraviolet.

**Key words:** galaxies: active – galaxies: formation – galaxies: individual (FSC 10214+4724) – galaxies: starburst – gravitational lensing

## 1 INTRODUCTION

The  $z = 2.286$  IRAS galaxy FSC 10214+4724 is one of the most apparently luminous objects in the Universe, and its discovery (Rowan-Robinson et al. 1991) led to much speculation about its possible status as a protogalaxy. This speculation was based on the extreme bolometric luminosity of the object (Rowan-Robinson et al. 1991), and more specifically on the huge gas mass and star formation rate inferred from the sub-mm molecular line and continuum detections (e.g. Solomon, Downes & Radford 1992; Rowan-Robinson et al. 1993).

This speculation was dampened by a series of pa-

pers which proved that F10214+4724 is being gravitationally lensed, and, at all wavebands, is intrinsically an order of magnitude or more dimmer than it first appeared. Although a lensing bias was suspected by a number of authors (e.g. Elston et al. 1994, Trentham 1995), the first direct empirical evidence of strong gravitational lensing was provided by a deep near-infrared image (Matthews et al. 1994) which revealed an arc-like structure centred on a galaxy close to the line of sight to F10214+4724. Several sets of authors published lensing interpretations (Graham & Liu 1995; Serjeant et al. 1995; Broadhurst & Lehár 1995) which were confirmed by the appearance of the HST image of Eisenhardt et al. (1996): this image con-

tained highly elliptical, high surface brightness features characteristic of strong lensing, as well as a clear counter-image. These papers also attempted to constrain the redshift of the system responsible for the gravitational lensing, our contribution (Serjeant *et al.* 1995) being spectroscopy of two galaxies projected  $\approx 1$  and  $\approx 3$  arcsec from F10214+4724. This work revealed tentative  $4000\text{\AA}$  breaks at  $z \simeq 0.90$  in both galaxies, later confirmed using fundamental plane arguments in HST imaging (Eisenhardt *et al.* 1996), and also tentatively supported by a weak absorption line at  $z = 0.893$  in the F 10214+4724 spectroscopy of Goodrich *et al.* (1996). The HST R-band image of F10214+4724 implies magnifications of  $\sim 100$  (Eisenhardt *et al.* 1996) in this waveband, but it now seems likely that differential flux magnification causes lower magnification factors for the more extended structure, as argued by several authors.

Gravitational lensing appeared to offer a compelling explanation for the extreme luminosity of FSC 10214+4724 (*e.g.*, Broadhurst & Léhar 1995). As a result, the IRAS galaxy is no longer so extreme in its properties: indeed, in many respects, it resembles local ultraluminous infrared galaxies and Seyfert-II galaxies. Nevertheless, both Downes *et al.* (1995) and Green & Rowan-Robinson (1996) argue for a bolometric magnification factor of  $\lesssim 10$  using arguments based on minimum black body sizes. FSC 10214+4724 remains one of the most intrinsically luminous objects in the Universe. The importance in this object still lies in studying whether high- $z$  hyperluminous activity, such as that seen in FSC 10214+4724, differs in all but scale from local objects, and in determining the relative contributions of the starburst and AGN components (Elston *et al.* 1994; Lawrence *et al.* 1993, 1994; Soifer *et al.* 1995; Goodrich *et al.* 1996; Kroker *et al.* 1996; Hughes, Dunlop & Rawlings 1997).

Prior to making the observations reported in this paper there had been no direct evidence for the presence of an embedded broad-line (*e.g.* Seyfert-I or quasar) nucleus in F10214 + 4724, although high ( $\approx 20$  per cent) rest-frame ultraviolet polarization (Lawrence *et al.* 1993; Jannuzi *et al.* 1995) suggested that one was present. This situation changed with the deep spectropolarimetry of Goodrich *et al.* (1996) showing clear broad lines in polarized light. This extended the close spectral similarities between F10214 + 4724 and Seyfert-II galaxies, specifically NGC1068, which was first remarked on by Elston *et al.* (1994).

Prior to our observations there had also been no reported detection of the narrow ( $\lesssim 200 \text{ km s}^{-1}$ ) emission lines expected from any star-forming activity in F10214 + 4724. A star-forming component is expected if the analogy with NGC1068 is to be complete. This situation also changed during the preparation of this paper. Using a novel imaging near-infrared spectrometer Kroker *et al.* (1996) presented evidence for spatially-extended narrow  $\text{H}\alpha$  emission just as ex-

pected if the Seyfert-II nucleus of F10214+4724 is accompanied by a circumnuclear starburst.

In this paper we present, analyse and interpret optical and near-infrared spectroscopy of IRAS FSC 10214+4724. The details of data acquisition and analysis are given in Section 2. In Section 3 we compare our results with previous and contemporaneous spectroscopic studies of F10214+4724. In Section 4 we interpret the data on the Seyfert-II emission line region including a discussion of optical depth effects on the resonance lines, and some modelling of the spectrum using the photoionisation code CLOUDY (*e.g.* Ferland 1993, 1996). In this section we reach conclusions about the Seyfert-II properties of F10214+4724 which differ significantly from those reached by previous studies. In Section 5 we interpret the data on the region responsible for the narrow ( $\lesssim 200 \text{ km s}^{-1}$ )  $\text{H}\alpha$  line seen in our near-infrared spectrum: this feature is likely to be a signature of star formation. In Section 6 we pass some concluding remarks on the nature of F10214+4724. Further data on galaxies foreground to F10214 + 4724 are given in Appendix A, and our attempts at identifying the weak emission line at  $2067\text{\AA}$  are discussed in Appendix B.

## 2 DATA ACQUISITION AND ANALYSIS

### 2.1 Optical spectroscopy

We observed F10214+4724 on the nights 1995 January 28 and 1995 January 30 with the ISIS spectrograph on the William Herschel Telescope (WHT) taking advantage of 0.7-arcsec seeing. We refer the reader to Serjeant *et al.* (1995) for full details of these observations. The spectrophotometry is in good agreement with the continuum measurements tabulated by Rowan-Robinson *et al.* (1993) as well as (accounting for slit losses) the line parameters of Goodrich *et al.* (1995). There are significant disagreements between our measurements and those tabulated by Elston *et al.* (1994) — their line fluxes are typically larger by a factor  $\sim 2$  — but these can plausibly be attributed to imperfect correction for the non-photometric observing conditions experienced by Elston *et al.* Neither the continuum, nor any of the emission lines are resolved spatially (with  $\approx 0.35$  arcsec pixels); limits on the extended line emission are discussed by Serjeant *et al.* (1995).

### 2.2 Near-infrared spectroscopy

We observed F10214+4724 on two occasions with the short (150mm) camera and  $3''$  (single pixel) slit of the  $62 \times 58$  InSb CGS4 array (Mountain *et al.* 1990) on the UKIRT. The slit was aligned at a position angle of  $90^\circ$ . The first of these observations, on 1992 February 5, used the  $75 \text{ lines mm}^{-1}$  grating to obtain a first-order spectrum centred near  $1.6\mu\text{m}$ ; a series of 30s

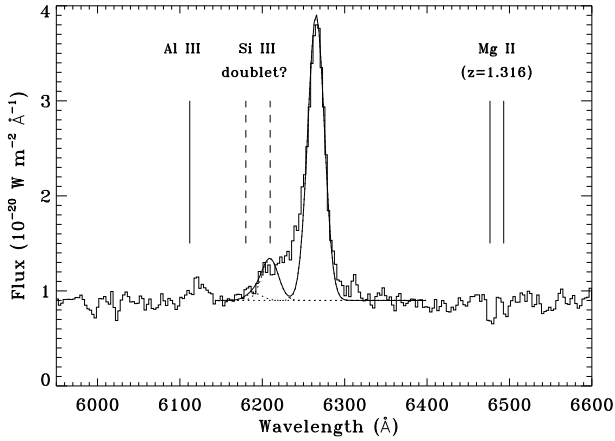


Figure 2: CIII] line modelled as a narrow line and narrow SiIII doublet. The individual model components are plotted as dotted lines, and the sum as a full line. Clearly this makes an extremely poor fit to the data. The positions of the AlIII emission line and the  $z = 1.361$  MgII absorber are also marked.

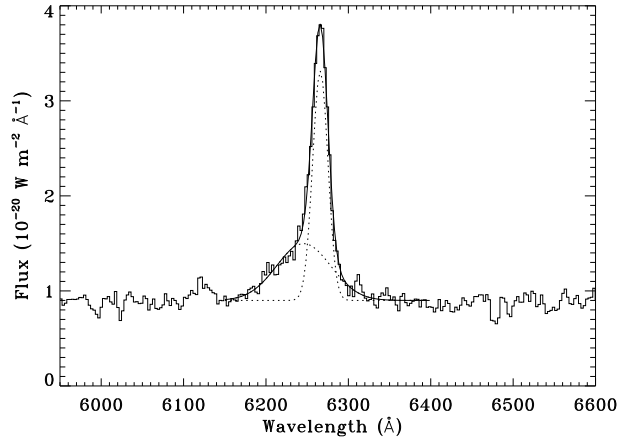


Figure 3: CIII] line modelled as two Gaussians.

exposures were arranged in sets of four shifted by 0, 0.5, 1 and 1.5 in wavelength — this provided Nyquist sampling and ensured that a given wavelength was sampled by two pixels. The standard ‘ABBA’ nodding pattern with a nod of 24 arcsec (8 detector rows) was used. The total exposure time was  $9 \times 4 \times 2 \times 30$ s for each point in the 126-pixel spectrum. The second observation, on March 23 1992, employed the 150 lines  $\text{mm}^{-1}$  grating to obtain a second-order spectrum centred near  $2.16\mu\text{m}$ . The nod in this case was  $30''$  (10 rows), and the total exposure time  $10 \times 4 \times 2 \times 40$ s per point. Spectra were wavelength calibrated using Xenon/Argon lamps and night-sky hydroxyl lines, flux calibrated using HD105601, and the positive and negative channels were extracted from their respective 3-arcsec wide rows. The wavelength calibration is accurate to  $\sim 0.003\mu\text{m}$  in H and  $0.001\mu\text{m}$  in K, and the spectral resolving powers were 250 at H and 1400 at K.

### 3 RESULTS AND COMPARISON WITH OTHER SPECTROSCOPY

#### 3.1 Optical spectroscopy

Figure 1 shows our WHT optical spectrum of F10214+4724; line fluxes, widths and redshifts are tabulated in Table 1. Deeper spectra covering the region above  $3900 \text{ \AA}$  have been presented by Soifer et al. (1995) and Goodrich et al. (1996), and an MMT spectrum, comparable in sensitivity and wavelength range to our data, is presented by Close et al. (1996); see also Rowan-Robinson et al. (1991) for the discovery spectrum. The velocity profiles of all the emission lines except Ly $\alpha$  are, with FWHMs around  $1000 \text{ km s}^{-1}$ , extremely similar. These line widths are small

compared to quasar broad lines, but large compared to typical AGN narrow lines which are typically a few hundred  $\text{km s}^{-1}$  (e.g. Nelson & Whittle 1996).

The accuracy of our wavelength calibration means that the identification of the bright doublet in the far blue with OVI is secure, and we are forced to conclude that Close et al. (1996) were mistaken in preferring Ly $\beta$  as the identification for this feature. This is probably the most clearly resolved example of the OVI doublet (see e.g. Kriss et al. 1992a,b; Laor et al. 1994), a factor we will exploit in Section 4. Above  $3900 \text{ \AA}$  comparison with the published spectra shows that all the labelled features are real. The identification of the (rest-frame)  $2470 \text{ \AA}$  feature, which is also seen in NGC 1068, is new but probably uncontroversial. The identification of the line at  $\approx 1805 \text{ \AA}$  is more uncertain: we have followed Lacy & Rawlings (1994) by identifying it with MgVI, a line present in the CLOUDY models discussed in section 4.2. A strong line at this wavelength is also seen in NGC 1068 (Snijders, Netzer & Boksenberg 1986). We prefer the MgVI identification to either the SiII  $1814.0 \text{ \AA}$  multiplet or the [NeIII]  $1814.6 \text{ \AA}$  line: these were suggested as possible identifications by Snijders et al., and adopted for F10214+4724 by Soifer et al. 1995 and Close et al. 1996. Note that the ionisation potential of  $\text{Mg}^{5+}$  is 141.2 eV, and thus even more extreme than the 113.9 eV required to produce  $\text{O}^{5+}$ .

This leaves one unidentified line at a rest-frame wavelength of  $2067 \text{ \AA}$ . This line is also seen in the HST spectrum of NGC1068 (Antonucci, Hurt & Miller 1994) where it lies in a region confused by underlying FeII multiplets (see also Wills, Netzer & Wills 1980 for a discussion of a  $2080 \text{ \AA}$  feature in the spectra of quasars), but in F10214+4724 it is clearly a distinct narrow feature. Our attempts at identifying this line are discussed in Appendix B.

The broad asymmetric base to the CIII]1909 line is shown in more detail in fig 3. This broad base independently present (though marginally) in both night’s

spectra. The data are reproduced by the sum of two Gaussian components with a broad ( $\sim 4000 \text{ km s}^{-1}$ ) component blueshifted by about  $1000 \text{ km s}^{-1}$  relative to a component with a similar FWHM (e.g.  $\approx 1000 \text{ km s}^{-1}$ ) to the other optical lines. Although lines of SiIII] are expected to be present at some level in the blue wing of CIII]1909 (see fig 2) we were unable to obtain as good a fit using a superposition of  $\approx 1000 \text{ km s}^{-1}$  lines (fig 2). This implies that the previous detection of hint of a broad CIII]1909 line in integrated light (Goodrich *et al.* 1996) is not attributable solely to the neighbouring narrow emission lines. There is also an apparent blue wing to the CII]2326 line, but this feature is sensitive to the correction for the atmospheric A band. The lack of broad components to other lines may be explainable by a combination of scattering albedo and reddening towards the scattering surface (or between the BLR and the scatterers, or within the scattering region itself); also lower signal to noise may mask broad features in the Ly $\alpha$  and NV region (figure 4).

The Ly $\alpha$  line has a number of unusual properties which have been noted by other authors. First, it is weak relative to the other ultraviolet emission lines, e.g. NV. This appears to reflect anomalously weak Ly $\alpha$  emission: ignoring Ly $\alpha$ , both NGC 1068 (e.g. Snijders *et al.* 1986, Kriss *et al.* 1992) and the IRAS-detected Seyfert 2 galaxy NGC 3393 (Diaz *et al.* 1988) have similar ultraviolet spectra to F10214+4724. Secondly the Ly $\alpha$  line is double peaked; this has been interpreted as requiring ‘self-absorption’ (Soifer *et al.* 1995; Close *et al.* 1996). We will discuss these points further in Section 4.

The continuum depression shortward of Ly $\alpha$  is within the range, though at the upper limit observed in quasars at similar redshifts (e.g. Warren *et al.* 1994), consistent with the expected lack of a QSO proximity effect (e.g. Giallongo *et al.* 1996 and refs. therein). The HeII1086 line may be marginally detected. We confirm the presence of a Mg II 2800 absorption doublet at  $z = 1.316$  (see fig 2), but have insufficient sensitivity to confirm the weaker  $z = 0.892$  doublet tentatively identified by Goodrich *et al.* (1996).

### 3.2 Near-infrared spectroscopy

Our H-band spectrum of F10214+4724 is shown in fig 5, and our K-band spectrum in fig 6. Other near-infrared spectroscopy of F10214+4724 has been published by Elston *et al.* (1994), Soifer *et al.* (1995), Iwamuro *et al.* (1995) and Kroker *et al.* (1996).

We obtain an approximate lower limit on the [OIII]4959+5007 to H $\beta$  ratio of 10. Iwamuro *et al.* (1995) claim a tentative detection of H $\beta$  with an OIII to H $\beta$  ratio of 27, though the H $\beta$  is a factor of 3 brighter than the upper limit quoted by Elston *et al.* (1995). Iwamuro *et al.* used the OH airglow suppressor spectrograph on the UH 2.2m, so their detection

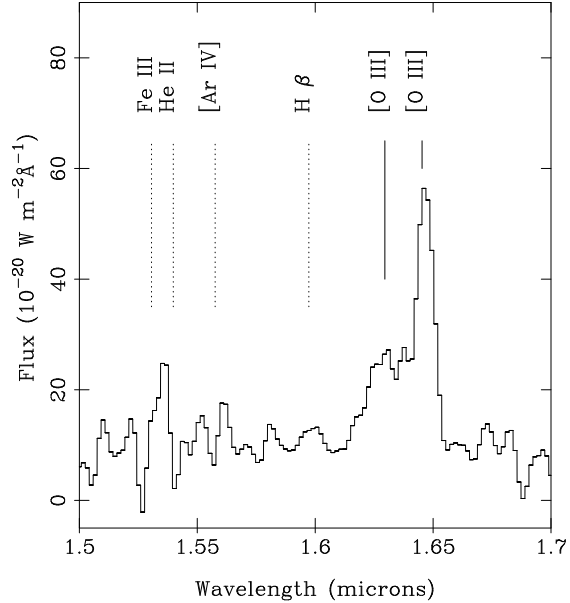


**Figure 5.** H band spectrum of F10214+4724. The position of the [OIII] doublet is marked, as are the predicted positions of other emission lines at  $z = 2.286$ .

should be less prone to difficulties in sky subtraction. However, it is not clear how imperfect sky subtraction could lead to an underestimate of the H $\beta$  flux without a corresponding null detection of the [OIII] 4959, 5007 $\text{\AA}$  doublet, since the sky lines are if anything stronger near the [OIII] lines, and the relative variations of the sky lines are typically  $\leq 10\%$  (Ramsey *et al.* 1992); there are also no strong atmospheric absorption lines in the vicinity, and the spatial variation of the sky spectrum is also expected to be negligible. Nevertheless, the lower resolution H band spectrum of Soifer *et al.* (1995) has a marginally detected blue wing to the [OIII] lines which may be H $\beta$ .

Weak features near the predicted position of the HeII4686 line appears to be present, which might contribute to the unusual width of the apparent 4686 line in Soifer *et al.* (1995). However, none of these features is reliably detected, and none lies on any of the positions of  $z = 2.286$  emission lines expected to be prominent (see e.g. section 4.4 below) which casts doubt on the reliability of the apparent detections. Soifer *et al.* (1995) quote a detection of HeII 4686 $\text{\AA}$  at an OIII/HeII ratio of 23, much fainter than the limit ( $\sim 5$ ) placed in figure 5; this detection is confirmed, albeit tentatively, by Iwamuro *et al.* (1995).

The H $\alpha$  line profile in our CGS4 K band spectrum (figure 6) is clearly resolved into a broader resolved component, with width comparable to the UV emission lines, and a narrower unresolved component of H $\alpha$  and [NII]. We fit the K band spectrum using the stsdas.fitting.ngauss package with the back-

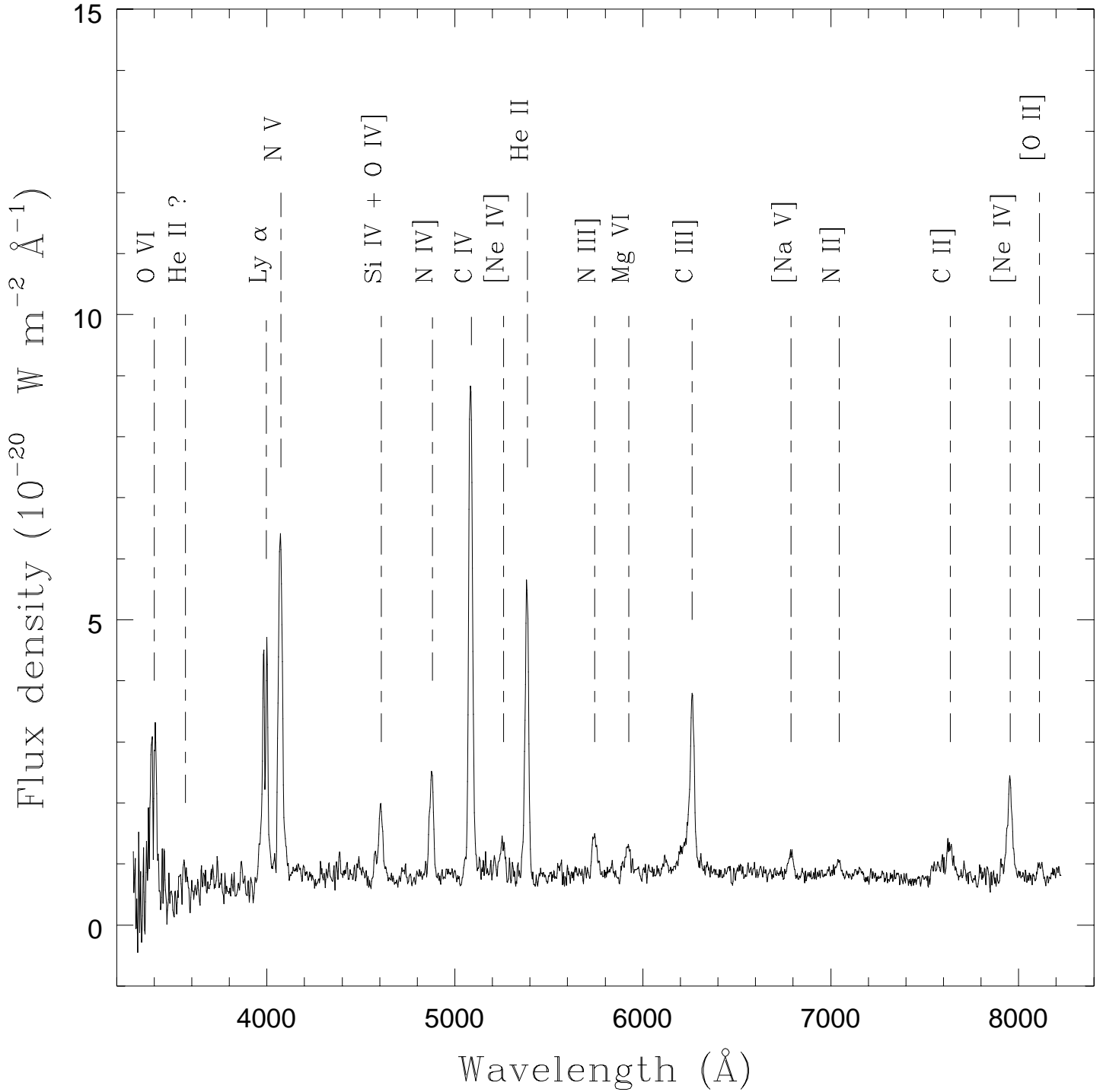


**Figure 1.** WHT spectrum of F10214 + 4724. The spectrum was extracted from a full width, zero intensity aperture, thereby ensuring accurate spectrophotometry. This also included some light from a nearby companion object, particularly redward of  $\approx 7500\text{\AA}$ , as discussed by Serjeant *et al.* (1995). The emission lines are marked with their

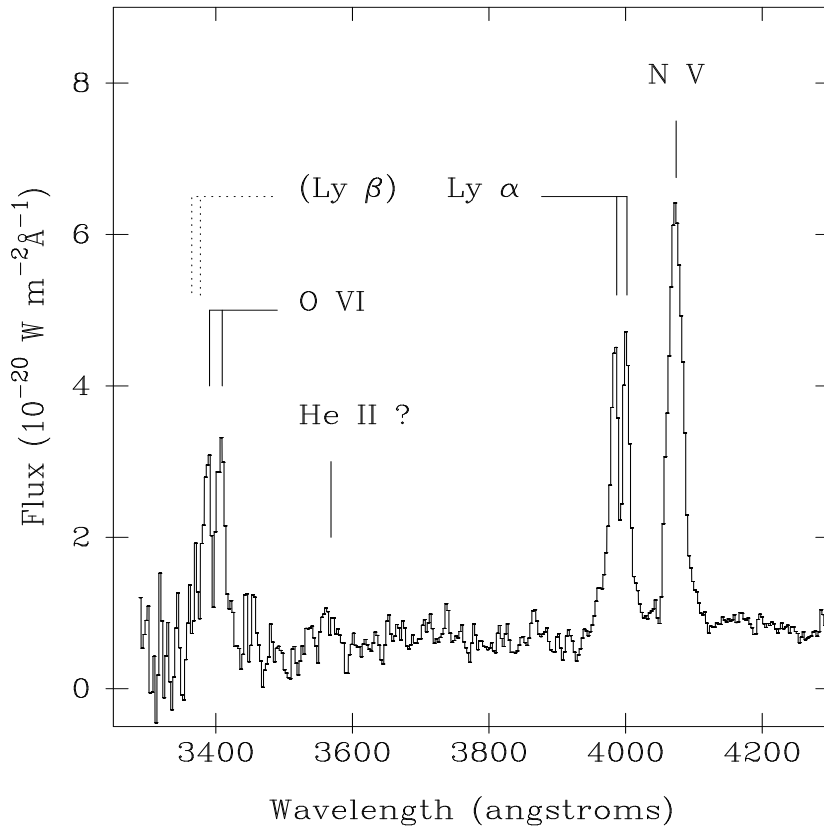


**Figure 4.** Expanded UV spectrum of F10214+4724. Positions of major emission lines are marked; also shown are the predicted positions of Ly $\beta$  associated with the observed Ly $\alpha$ .

ground level as a free parameter, and with the following four gaussians: first, three unresolved (FWHM  $200 \text{ km s}^{-1}$ ) gaussians to model the narrower H $\alpha$  line and satellite [NII] 6548, 6584Å lines, with the 6548 component constrained to have the same redshift and 1/3 the flux of the 6584; second, a further gaussian with unconstrained amplitude, position and width. Although the broader component is a blend of the broader H $\alpha$  and satellite [NII] lines, we model it as a single Gaussian for simplicity.

The results, displayed in figure 7, were very similar to a deblending with 3 Gaussians of unconstrained position and width, and further deblending models with alternative simplifying assumptions were attempted. In particular, the region between the narrower H $\alpha$  and the narrower [NII]6584 lines was very poorly fit in models without a broad excess, as might be expected from figure 7. The flux in this region is clear evidence for an additional component. From the variations in the narrower line flux between the models we estimate the flux errors in both the narrower H $\alpha$  and [NII]6584Å lines to be  $\leq 30\%$  (table 1). The

flux from the broader H $\alpha$  component (distinct from [NII]) is very poorly constrained.

Note that although the narrower H $\alpha$  line is unresolved (FWHM less than  $\sim 200 \text{ km s}^{-1}$  at a resolving power of 1428), there is marginal evidence that the [NII] 6584Å line is resolved. We found that at least some of the apparent excess on the [NII] line, if real, may be attributable to the broader [NII] component. If we assume that the satellite lines contribute 60% of this flux, we obtain a broader H $\alpha$  flux of 75% of the total H $\alpha$ . Note that the model does not imply the narrowest lines are Gaussian, but rather that the K-band spectrum must have at least one unresolved and at least one resolved component. This is exactly as expected for a hybrid starburst / AGN system.

To summarise, we find three distinct kinematic components in our new spectra of F10214+4724: a  $\sim 1000 \text{ km s}^{-1}$  component, present in H $\alpha$  and in the UV lines which comes from the Seyfert-II Narrow-Line Region as will be discussed further in Section 4; a  $< 200 \text{ km s}^{-1}$  component, present in H $\alpha$ , which we chose to associate with starburst activity, as will be discussed in Section 5; and a  $4000 \text{ km s}^{-1}$  CIII]1909

**Table 1.** Measurements from the WHT spectrum of F10214 + 4724.

Line Line	Position /Å	Redshift	EW / Å	Line flux /10 <sup>-19</sup> W m <sup>-2</sup>	Accuracy	Line width kms <sup>-1</sup>	Comments
O VI 1031.9	3388	2.283	60	4.5	30%	1200–1600	
O VI 1037.6	3408	2.284	60	4.3	30%	500–1200	
CIII? 1175.7	3866	2.288	6	0.4	60%		
Lyα 1215.7	3987	2.279	45	5.3	30%	0–900	two Gaussian
Lyα 1215.7	4002	2.292	40	4.7	30%	0–600	fit poor
N V 1240.1	4074	2.285	130.0	14	20%	1500–1700	doublet marginally resolved
CII 1335.3	4390	2.288	4	0.3	60%		
Si IV 1393.7	4577	2.284	8	0.7	50%		
O IV] 1402.5	4607	2.285	40	3.3	30%	1300–1500	blended with Si IV 1402.8
N IV] 1486.5	4879	2.282	45	4.0	25%	1250–1450	
C IV 1549.0	5087	2.284	150	19.0	20%	900–1200	
[Ne IV] 1602.0	5257	2.282	10	1.1	40%	1000–1200	
HeII 1640.5	5385	2.283	100	10.0	20%	800–1150	
N III] 1750	5743	2.282	20	2.0	30%	1200–1350	
Mg VI 1806	5924	2.280	15	1.5	40%	1200–1350	
Al III 1857.4?	6104	2.286	5	0.5	60%		Unidentified red wing
C III] 1908.7 narrow	6267	2.283	60	6.5	30%	800–1000	
C III] 1908.7 broad	6244	2.271	35	5.3	40%	≈3700	
[Na V] 2068	6791	2.265	10	1.2	40%	1000–1150	see text
N II] 2142.8	7045	2.287	8	0.8	50%	950–1100	blend with Si VII 2148 ?
C II] 2326.3	7638	2.284	30	3.0	40%	≈1500	blend with OIV 2321 ?
[Ne IV] 2422.0	7955	2.284	40	5.2	30%	900–1050	
[O II] 2470.3	8115	2.285	12	0.8	30%	1000–1150	
[O III] 4959	16279	2.283	280	23.4	30%	< 1300	
[O III] 5007	16453	2.286	580	49.8	30%	< 1300	
[N II] 6584	21634	2.286	14	6.6	30%	<200	
Hα	21564	2.286	12	5.5	30%	<200	
Hα+[N II] broad	21585	~ 2.28	83	38.3	20%	~ 1800	not deblended

Notes to Table 1: Errors on the line fluxes represent ~90 % confidence intervals expressed as a percentage of the best line flux estimate; for the strongest lines these are dominated by roughly equal contributions from uncertainties in fixing the local continuum level, and from the absolute flux calibration. Line widths were estimated from the FWHM of the best Gaussian fit to each line; for the rest-frame UV lines, the range lower value assumes that the line-emitting region fills the 2 arcsec WHT slit, the higher value that it is broadened only by the seeing.

line which originates in a hidden Seyfert-I, or quasar, nucleus as has been discussed by Goodrich et al. (1996).

## 4 THE SEYFERT-II NARROW-LINE REGION

### 4.1 Resonant scattering of Lyman series lines

There is strong evidence for resonant scattering of the Lyα emission line: the profile of Lyα is double peaked, and the peaks are symmetrically displaced about the predicted position of Lyα at  $z = 2.286$  with equal flux (within the errors; table 1). If the Lyα-emitting region is free of dust then the velocity shift  $v$  of either Lyα peak from 1215.7Å is given by:

$$v = 195 \left( \frac{N_H}{10^{24} \text{m}^{-2}} \right)^{1/3} \left( \frac{T}{10^4 \text{K}} \right)^{1/6} \text{ km s}^{-1} \quad (1)$$

(Neufeld & McKee 1988), where  $N_H$  is the total atomic hydrogen column density to the source of the Lyα photons, and  $T$  is the gas temperature. The measured velocity separation of the peaks is  $2 \times \sim 560 \text{ km s}^{-1}$  yielding  $N_H = 2.5 \times 10^{25} \text{ m}^{-2}$  for  $T = 10^4 \text{ K}$ .

The total line-centre optical depth to the source of the Lyα photons is  $\tau_{\text{Ly}\alpha} \sim N_H \times k_{\text{Ly}\alpha}$  where  $k_{\text{Ly}\alpha}$  is the absorption cross-section to the line centre of Lyα. In the general case of photon absorption promoting an electron upwards in energy from level  $i$  to level  $j$ , the line-centre cross-section  $k_l$  is given by

$$k_l = \frac{1}{4\pi\epsilon_0} \frac{\sqrt{\pi} e^2 f_{ij}}{mc\Delta\nu_D} \quad (2)$$

where  $f_{ij}$  is the oscillator strength for the transition,  $m$  and  $e$  are the electronic mass and charge,  $c$  is the speed of light and  $\epsilon_0$  is the vacuum permittivity;  $\Delta\nu_D = \left( \frac{2kT}{M_A c^2} \right)^{0.5} \times \nu_0$  is the Doppler width of the line with  $\nu_0$  the central frequency,  $k$  the Boltzmann constant and  $M_A$  the atomic mass. In the case of the

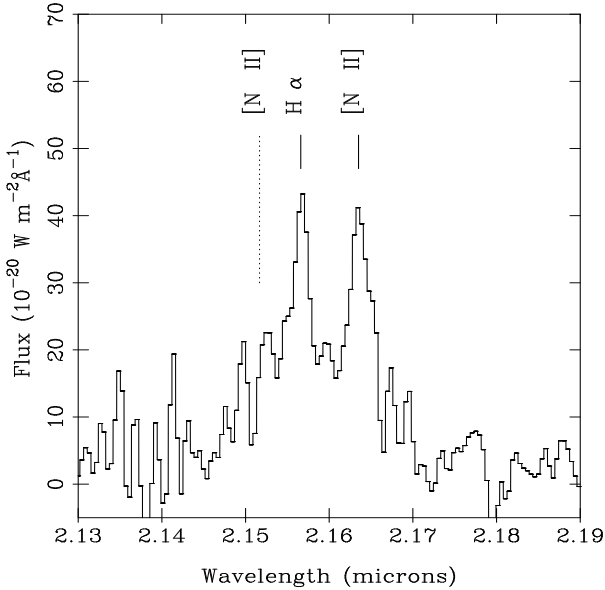


**Figure 6.** K band spectrum of F10214+4724. The position of the narrower H $\alpha$  and [NII] 6584Å lines are marked assuming  $z = 2.286$ , as is the predicted position of the [NII] 6548Å line. Note the clear broad base to these lines.

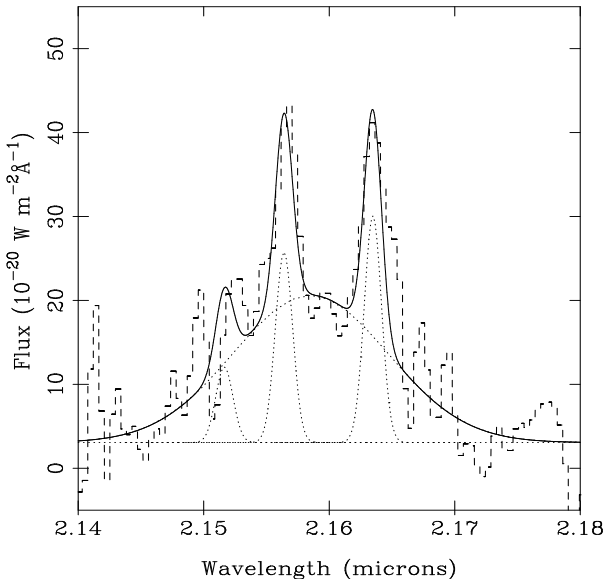


**Figure 7.** Fit to the K band spectrum of F10214+4724 discussed in the text.

Ly $\alpha$  line, taking  $T = 10^4$  K, these equations yield  $k_{\text{Ly}\alpha} = 5.8 \times 10^{-18} \text{ m}^2$ , and thus  $\tau_{\text{Ly}\alpha} = 1.5 \times 10^8$ .

Resonant scattering is extremely efficient at removing Ly $\beta$  photons even at moderate optical depths (*e.g.* Netzer 1975, Osterbrock 1989), in agreement with the null detection of Ly $\beta$  in F10214+4724. The strong influence of resonant scattering on the observed properties of the Lyman series lines is a major difference between the spectroscopic properties of F10214+4724 and NGC 1068. Ultraviolet spectroscopy of the latter (Kriss *et al.* 1992) shows a strong single-peaked Ly $\alpha$  line as well as Ly $\beta$ ; the observed Ly $\beta$  / Ly $\alpha$  flux ratio of 0.12 implies  $\tau_{\text{Ly}\alpha} \lesssim 10$ .

Is this neutral material within the narrow line region, or external, such as a damped Ly $\alpha$  system associated with the host galaxy? The QSO proximity effect (*e.g.* Giallongo *et al.* 1996) suggests that neutral material is often destroyed within the ionisation cone. If the  $N_H$  is associated with the host, it need not cause damped absorption in F10214 itself (countering the most obvious criticism), because the geometry would allow scattering into the line of sight. This neutral hydrogen could be intrinsic to the host, or could be the result of accretion of gas-rich dwarfs; neutral systems with column densities  $\geq 10^{25} \text{ m}^{-2}$  are known to undergo a strong cosmological evolution which dominates the evolution in  $\Omega_g$  (Wolfe *et al.* 1995).

Can the  $N_H$  gas:dust ratio, derived from the Ly $\alpha$  strength, be used to resolve this? Ly $\alpha$  photons are conserved in resonant scattering, but the Ly $\alpha$  strength can be suppressed by dust absorption between scatterings. The predicted case B Ly $\alpha$  flux from our broader H $\alpha$  flux implies a suppression factor of  $< 10^2$ , the limit assuming no [NII] 6548, 84. In the damped Ly $\alpha$  models of Charlot & Fall (1991), a neutral screen with velocity dispersion  $10 \text{ km s}^{-1}$  and column density as derived above yields a Ly $\alpha$  suppression of  $\sim 10^4$ , but if the gas:dust ratio is  $\sim 4$  times lower than the values typically inferred from the reddening of quasars with damped systems this can be reconciled with our observed Ly $\alpha$ . The Ly $\alpha$  flux therefore cannot exclude the possibility of a damped system associated with the host. Alternatively, the same models predict a suppression  $\sim 10^{-1}$  for sources distributed throughout the  $N_H$  (for a velocity dispersion of  $1000 \text{ km s}^{-1}$  the suppression becomes only  $\sim 0.75$ ), and the authors argue that geometrical factors could reduce this to unity.

There are difficulties with resonant scattering within the narrow line region: the clouds in the nearer ionisation cone suffer resonant scattering, but we nevertheless ought to have an unobscured view of the clouds in the more distant ionisation cone. The contradicts *e.g.* the observed lack of Ly $\beta$ , but this could be explained by differential magnification of the nearer ionisation cone, or selective obscuration of the more distant ionisation cone *e.g.* by the host galaxy.



We nevertheless favour models with at least some of the neutral column in the rear of the narrow line clouds themselves, since the photoionisation models below (section 4.2) favour ionisation-bounded clouds. Higher resolution K-band spectroscopy may resolve the AGN H $\alpha$  from the satellite [NII] lines, and the inferred Ly $\alpha$  suppression may exclude the damped system model. Spatially resolved spectroscopy of F10214+4724 (while subject to the uncertainties in the projection to the source plane) may provide a further confirmation: diffuse Ly $\alpha$  could be used to trace any extended neutral hydrogen (Villar-Martin *et al.* 1996), modulo the uncertainties in the projection to the source plane. The detection of non-resonance lines spatially coincident with any extended Ly $\alpha$  would rule out resonance scattering “mirrors” and identify such emission with the AGN narrow line region or starburst knots.

#### 4.2 Photoionisation models

If we exclude the resonantly scattered Ly $\alpha$ , the marginally resolved doublet NV1240, 1243, and the blended emission lines (labelled in table 1), then we find no correlation of ionisation potential with emission line width. As a result we may attempt to model the emission line spectrum with constant density single slab photoionisation models, at least to first order.

We modelled the Seyfert-II lines with the photoionisation code CLOUDY (version 84.12, Ferland 1993), assuming for simplicity that the rest frame UV emission lines in F10214+4724 suffer zero extinction (section 4.4). Unless otherwise stated, we used an AGN ionising continuum as characterised by Matthews & Ferland (1987) with a break at 10 $\mu$ m (see Ferland 1993). We considered hydrogen densities  $8 \leq \log_{10} n \leq 16$ , where  $n$  is the total hydrogen column density (*i.e.* molecular, neutral and ionised) in units  $\text{m}^{-3}$ , and ionisation parameters  $-4 \leq \log_{10} U \leq 0$ , where  $U$  is the dimensionless ratio of incident ionising photons to hydrogen density, *i.e.*  $U = \Phi(H)(nc)$ . Here  $\Phi$  is the surface flux of ionising photons in  $\text{m}^{-2}\text{s}^{-1}$ , and  $c$  the speed of light. The calculation was stopped at a column density of  $10^{27} \text{ m}^{-2}$ , or at a temperature of 4000K, since below this temperature the emission line flux is negligible. We used the default solar metallicity (see Ferland 1993), and CLOUDY assumes a plane-parallel geometry.

The HeII:Ly $\alpha$ :OVI:CIV ratios are sensitive to the UV-soft Xray continuum (*e.g.* Krolik & Kallman 1988), so are sensitive to the presence or absence of an active nucleus. A black body ionising continuum at 40,000K, resembling the continuum from the hottest OB stars, as severe difficulty in producing OVI1032, 1037 $\text{\AA}$  or MgVI 1806 $\text{\AA}$ , due to the extremely high ionisation potentials of O $^{4+}$  and Mg $^{4+}$  (.11 and .14 keV respectively). The AGN ionising continuum defined above had no difficulty in reproducing these lines. We are therefore confident that the  $\sim 1000$

km s $^{-1}$  emission line region is predominantly photoionised by the active nucleus.

None of the single-slab models provided an adequate fit to all the rest-frame UV emission lines. We found that similar, but not identical, conditions ( $\log_{10} n \sim 10$ ,  $\log_{10} U \sim -1.5$ ) were implied by emission lines [NeIV] 1602, HeII 1640, NIV] 1486, NIII] 1750, Nev 3426, NeIII 3869. For example, the largest [NeIV] 2424 / HeII 1640 ratio in our models was with a density and ionisation parameter of  $\log_{10} = 10$ ,  $\log_{10} U = -1.4$ . This underpredicts the OVI and MgVI lines, as well as the N lines. However, the NIII] 1486, 1750 and NV1240 ratios are all consistent with  $\log_{10} U \sim -1.25$ ; this self-consistency of the N lines suggests that the strength of the N 1240 $\text{\AA}$  line may be due mainly to an abundance effect, as also argued in the IRAS detected Seyfert II NGC 3393 (Diaz *et al.* 1988) rather than due to differential magnification (Broadhurst & Léhar 1995). If so, this would further reduce the proportion of H $\alpha$  in the broader component of figure 7.

This model reproduced the CIV:CIII] ratio, but overpredicted their strength by  $\sim \times 5$ . A low carbon abundance ( $\sim 0.5 \times$  solar) might resolve the anomaly, perhaps caused by depletion onto dust grains. Much more problematic is the lack of an [OIII] 1665 $\text{\AA}$  emission line, which in these conditions should have a flux  $\sim 10\%$  of HeII 1640 $\text{\AA}$ . There does not appear to be any simple solution; we note however that an identical problem was found by Kriss *et al.* (1992b) in NGC1068, who argued that shock-heated gas would also produce the [OIII] 1665 line.

Finally, we can use our limits on the density and ionisation parameter to derive the sizes and masses of the NLR clouds. The clouds are ionisation bounded in the conditions we derived from the emission line ratios, as is also conventionally assumed for AGN narrow line regions, and unlike *e.g.* the matter-bounded extended emission line region models of Wilson *et al.* 1997. This supports our model for the resonant scattering (section 4.1), and is also consistent with the presence of [OI] in the Keck spectrum (Soifer *et al.* 1995). Assuming the absorbing column does indeed occur within the NLR clouds (assumed constant density for simplicity), we obtain a characteristic size scale of

$$S = N_H/n_H = 2.5 \times 10^{-2 \pm 0.5} \text{pc} \quad (3)$$

where the errors represent the acceptable range in the models, rather than *e.g.* gaussian noise. The mean mass of the NLR clouds is given by

$$M = u \times n_H \times S^3 = 1 \times 10^{-2 \pm 1} M_\odot \quad (4)$$

Unfortunately it is not possible to derive a covering factor or volume filling factor, without spatially resolved spectroscopy. Briefly,  $N$  clouds with covering factor  $C$  at mean distance  $D$  parsecs from a luminosity  $L$  quasar, are indistinguishable from  $N, C/4, 2D, 4L$ . We can however estimate the num-

ber of narrow line clouds, and the total cloud mass contained in the narrow line region. Using CLOUDY, we find the emissivity of a single cloud of density  $10^{10.5 \pm 0.5} \text{ m}^{-3}$  with ionisation parameter  $10^{-1.25 \pm 0.25}$  in *e.g.* the HeII 1640 line is  $\epsilon = 10^{-2.4 \pm 0.7} \text{ W m}^{-2}$ . For a magnification factor of  $10\mathcal{M}_{10}$ , our observed line flux implies the number of narrow line clouds is

$$\begin{aligned} N &= (10^{-18} \text{ W m}^{-2} \times 4\pi D_L^2) / (4\pi\epsilon S^2 \times 10\mathcal{M}_{10}) \\ &= 1 \times 10^{7 \pm 1.4} \mathcal{M}_{10}^{-1} h_{50}^{-2} \end{aligned} \quad (5)$$

where  $D_L$  is the luminosity distance to F10214+4724, given (assuming  $\Omega_0 = 1$ ,  $\Lambda = 0$ ,  $H_0 = 50 h_{50} \text{ km s}^{-1} \text{ Mpc}^{-1}$ ) by

$$D_L = 0.04 ch_{50}^{-1} (1 - (1 + 2.286)^{-0.5}) (1 + 2.286) \quad (6)$$

(We also note that variations in  $S$  correlate with variations in the cloud emissivity, so the “errors” do not simply add). The inferred total mass of ionised gas within the narrow line region is consistent with estimates in local AGN (*e.g.* Osterbrock 1993):

$$\begin{aligned} NM &= 10^{-18} 4\pi D_L^2 n_H S^3 / (4\pi S^2 \epsilon 10\mathcal{M}_{10}) \\ &= N_H \times 5 \times 10^{12 \pm 0.7} \text{ m}^2 \mathcal{M}_{10}^{-1} h_{50}^{-2} \text{ kg} \\ &= 2 \times 10^{5 \pm 0.7} \mathcal{M}_{10}^{-1} h_{50}^{-2} M_\odot \end{aligned} \quad (7)$$

Our choice of HeII, while free of metallicity effects, assumes negligible extinction (section 4.4) which will be testable with higher quality infrared spectra. Note that if spatially resolved spectroscopy detects the emission line counterimage, it may be possible to determine  $\mathcal{M}_{10}$  independently of spatial structure in the IRAS galaxy. As a corollary to the covering factor calculation one may then also obtain a robust estimate of the luminosity of the obscured quasar (Goodrich *et al.* 1996).

### 4.3 Optically-thick OVI emission

The resonant OVI 1034, NV 1240 and CIV 1549 lines are doublets in the isoelectronic lithium sequence. If such lines emanate from a region which is optically-thin to resonant scattering, then their doublet line ratios are given by the ratio of the statistical weights of the upper levels, *i.e.* 2:1 with the lower wavelength line of the doublet the brighter. However, in optically-thick regions, photon trapping and collision de-excitation can cause the levels to thermalize so that the flux ratio approaches  $\sim 1:1$ ; this thermalization occurs only at high values of optical depth and electron density  $n_e$ , namely when  $n_e \tau_0 \gtrsim 10^{22} \text{ m}^{-3}$  (Hamann *et al.* 1995). A doublet ratio of 1:1 therefore implies extreme densities and/or optical depths.

The OVI 1031.9, 1037.6 doublet in F10214+4724 is clearly resolved (Fig. 4), and its flux ratio 1:1 suggests line thermalization. We first consider whether this ratio is strongly influenced by blanketing by the Ly $\alpha$  forest lines — both a simple empirical test and a brief analytical argument suggest it is not. The test involved fitting low-order polynomials to the UV continuum longward of Ly $\alpha$ , and extrapolating these fits

to shorter wavelengths to estimate the level of line blanketing. We then superimposed a model 2:1 doublet at several positions on this absorption spectrum and found it impossible to obtain an apparent 1:1 ratio. This is in good agreement with the following analytical argument. The number of Ly $\alpha$  forest lines per unit redshift per unit rest-frame equivalent width is well fitted by an expression of the form

$$\frac{d^2 N}{dz dW} = \frac{A_0}{W^*} (1+z)^\gamma \exp\left(-\frac{W}{W^*}\right) \quad (8)$$

where  $\gamma \simeq 1.89$ ,  $W^* \simeq 0.27 \text{ \AA}$  and  $A_0 \simeq 10$  (*e.g.* Bechtold 1994). By integrating this over the redshift range 1.770 to 1.792 (*i.e.* in the neighbourhood of the doublet and exactly encompassing the width of either line of the doublet), and further integrating  $dN/dW$ , it can be shown that a maximum of two Ly $\alpha$  forest lines are expected to lie on the position of one OVI line. In order for a 2:1 doublet to be suppressed to 1:1, the line blanketing over the shorter wavelength line must be approximately a factor of 2 (in addition to the mean blanketing); the probability of this occurring is negligibly small, a conclusion which is insensitive to the uncertainties in  $\gamma$ ,  $W^*$  and  $A_0$ .

This seems to imply that the OVI emitting region in F10214+4724 is both optically thick ( $\tau_{\text{OVI}} \gg 1$ ) and dense enough for the doublet to have become thermalised, *i.e.*  $n_e \tau_{\text{OVI}} \gtrsim 10^{22} \text{ m}^{-3}$ . We will next show in the that the optical depth  $\tau_{\text{OVI}}$  is unlikely to exceed  $10^6$ , resulting in apparent broad-line-region-like conditions for the narrow OVI emitting region.

The latest release of CLOUDY (version 90.03a, Ferland 1996) incorporates the OVI 1032, 1037 $\text{\AA}$  doublet lines separately, so we used this code to explore the doublet ratios and OVI optical depths for a wide range of physical conditions. We used the same AGN ionising continuum, metallicity and stopping conditions as above. The results are shown in fig. 8. We find that the 1:1 ratio, also where the  $n_e \tau_0 \gtrsim 10^{22} \text{ m}^{-3}$  limit applies, is possible only with hydrogen densities in excess of  $n_H \simeq 10^{17} \text{ m}^{-3}$ . This conclusion was found to apply equally to  $N_H = 10^{26} \text{ m}^{-2}$  column and/or  $Z = 10Z_\odot$  metallicity gas. Such a high value of  $n_H$  is characteristic of the broad-line region of AGN (*e.g.* Ferland *et al.* 1992) rather than the lower values ( $n_e \sim 10^{11} \text{ m}^{-3}$ ) found in classical narrow-line regions.

Such a radical conclusion can be avoided, albeit with some fine tuning, by considering the Ly $\beta$  resonant absorption. This absorption is likely to be saturated, so the OVI doublet may lie inside its damping wings. Using the  $N_H$  value derived above, we obtain an optical depth of about 0.3 for the 1032 $\text{\AA}$  line and 0.09 for the 1038 $\text{\AA}$  line (*i.e.* a factor  $\sim 3.6$ ). To obtain a 1 : 1 ratio from 2 : 1, one needs an optical depth of around 1 to the 1032 $\text{\AA}$  line, close to the estimate from the observed  $N_H$ . This explanation avoids the high densities, but is sensitive to the assumed neutral

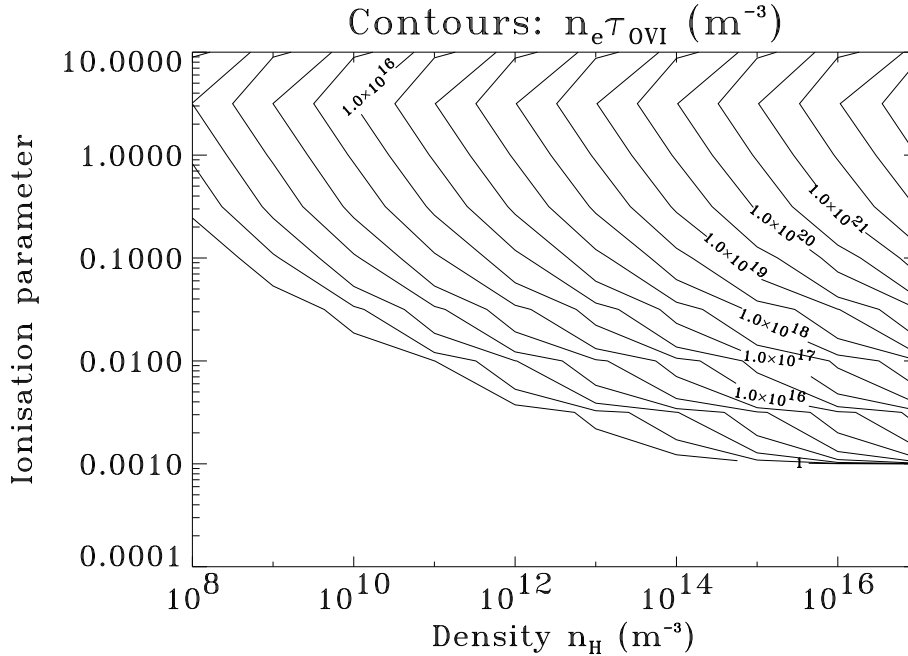


**Figure 8.** Results of the photoionisation model discussed in the text. The contours show the product of the  $n_p$ -weighted average electron density and OVI 1032+1037Å optical depth,  $n_e \times \tau_{\text{OVI}}$ , as functions of ionisation parameter and density. (Almost identical results were obtained replacing this  $n_e$  with the innermost zone electron density, the outermost, or the total Hydrogen density.) The contours are spaced logarithmically in steps of 0.5. Only where  $n_e \times \tau_{\text{OVI}} \gtrsim 10^{22} \text{ m}^{-3}$  does the OVI doublet form a 1:1 ratio.

column, and furthermore takes no account of geometrical effects (Vilar-Martin *et al.* 1996).

Inspection of the ultraviolet spectrum of NGC1068 (Kriss *et al.* 1992) suggests that the OVI doublet is again in a  $\sim 1:1$  flux ratio. However, there is no evidence of resonant scattering in this object.

#### 4.4 Reddening of the Seyfert-II nucleus

We can place limits on the extinction in the observed UV from the HeII 1640Å/HeII 1086Å ratio, which in the absence of reddening is predicted to be 7 (*e.g.* Seaton 1978). Although the signal to noise shortward of Ly $\alpha$  in Fig. 4 is poor, and despite possible blanketing by Ly $\alpha$  forest lines, the HeII 1086Å line is marginally detected at  $(\sim 7 \pm 50\%)^{-1}$  times the flux of the 1640Å counterpart. If real, this suggests an extinction of between zero and 0.75 magnitudes around 1200Å in the rest frame of F10214+4724 (*i.e.*  $A_V < 0.2$ ), or 2600Å in that of the lens (*i.e.*  $A_V < 0.4$ ). We can also obtain a rough extinction estimate from the H $\alpha$ :HeII1640Å ratio, predicted to be about 2.3 in our solar metallicity models above. We find (H $\alpha$ + [NII]):HeII=3.8, consistent with an H $\alpha$ :NII ratio resembling *e.g.* NGC 1068 (*e.g.* Bland-Hawthorn *et al.* 1991) and zero extinction.

Comparison of the *H* band detection of the HeII 4686Å line (*e.g.* Soifer *et al.* 1995) with the 1640Å line suggests extinctions  $A_V \sim 1.3$ . However, our photoionisation models above found the FeII4658Å

and/or ArIV4720Å lines can contribute up to three times the flux of the HeII4686Å line in densities of  $10^{10} - 10^{12} \text{ m}^{-3}$ , not unreasonable for AGN narrow line regions. Moreover, the Soifer *et al.* *H*-band spectrum has very low spectral resolution, and the HeII 4686Å line flux must be treated with some caution.

This low reddening in the rest-frame UV is in marked contrast to the high ( $A_V \geq 5$ ) rest frame optical extinction derived from Balmer decrements (*e.g.* Soifer *et al.* 1995), which led several authors to infer that at least two physically distinct regions contribute to the observed emission line spectrum (*e.g.* Elston *et al.* 1994, Soifer *et al.* 1995). The limit on the Balmer decrement of H $\alpha$ :H $\beta \geq 20$  reported by Elston *et al.* (1994) is at least in part resolved by our *K*-band spectrum. The narrower H $\alpha$  component contributes  $\sim 25\%$  of the total H $\alpha$  flux.; furthermore our total H $\alpha$  flux is  $\sim 25\%$  lower than that reported by Elston *et al.*, though this is within their stated photometric errors. However, this still yields  $A_V > 4$  in the frame of F10214+4724, or  $A_V > 6$  in that of the lens. (Any  $< 200 \text{ km s}^{-1}$  H $\beta$  leads to even higher  $A_V$ .) Alternatively, if we assume the Iwamuro *et al.* (1995) H $\beta$  detection is correct, the data are consistent with zero extinction. Further near-infrared spectroscopy is required to resolve this issue. We conclude that as yet there is no conclusive evidence for any significant reddening of the Seyfert-II nucleus.

## 5 STARBURST PROPERTIES

Our limit on the width of the narrowest  $H\alpha$  component in F10214+4724 is suggestive of a star-forming region as has previously been suggested by Kroker et al. (1996). Moreover, the fluxes of the [O I] 6300Å and [S II] 6724Å lines (Soifer et al. 1995) relative to the narrowest  $H\alpha$  component are similar to both those seen in spectra of local starburst galaxies (e.g. De Robertis & Shaw 1988) and in high luminosity IRAS galaxies (e.g. Leech et al. 1989). We can obtain an estimate of the star formation rate  $R$  from the narrower  $H\alpha$  line flux  $S$ , using the following expression adapted from Kennicutt (1983):

$$R(z = 2.286) = \frac{S(H\alpha)h_{50}^{-2}}{3 \times 10^{-21} \text{ W m}^{-2}} M_{\odot} \text{ yr}^{-1} \quad (9)$$

We assume a Hubble constant of  $H_0 = 50 h_{50} \text{ km s}^{-1} \text{ Mpc}^{-1}$  with  $\Omega_0 = 1$ ,  $\Omega_{\Lambda} = 0$ . If we assume the starburst region undergoes a net gravitational magnification of  $\mathcal{M} \lesssim 10$  (Downes et al. 1995, Green & Rowan-Robinson 1996, Graham et al. 1995), and that aperture corrections are negligible, we obtain a star formation rate of  $\gtrsim 20h_{50}^{-2} M_{\odot}$  per year. This corresponds to a starburst luminosity of  $\gtrsim 2.6 \times 10^{11} h_{50}^{-2} L_{\odot}$  (e.g. Moorwood 1996), i.e.  $\sim 0.5\%$  of the magnification-corrected bolometric power output.

Reddening by intervening dust would further increase this estimate of the star formation rate. Radiative transfer models of F10214+4724 (Green & Rowan-Robinson 1996) suggest a much larger starburst bolometric fraction of  $\sim 0.2 - 0.4$ , with a high starburst UV optical depth of  $\tau_{UV} \sim 800$ , i.e. an  $A_V \sim 160$ . Assuming this dust is well mixed with the  $H\alpha$  emitting gas (e.g. Thronson et al. 1990), the extinction and star formation rate is quite consistent with our observed narrow  $H\alpha$  flux, which for this  $A_V$  yields a starburst bolometric fraction of  $\sim 0.5$ . In both NGC1068 (Green & Rowan-Robinson 1996) and F10214+4724, the starburst and active nuclei appear to make comparable contributions to the bolometric power output.

## 6 CONCLUDING REMARKS

The presence of the optically thick OVI 1032, 1037Å doublet appears at face value to imply extremely high densities for narrow emission line gas,  $n_H \gtrsim 10^{17} \text{ m}^{-3}$ . However, we argue that it is more easily attributable to the Ly $\beta$  damping wings of resonant scattering material, probably within the AGN narrow line region. Differential magnification appears to play a significant role in the emission line spectrum of F10214+4724, in which we identify three distinct kinematic components: quasar broad lines ( $\sim 4000 \text{ km s}^{-1}$ ), Seyfert II narrow lines ( $\sim 1000 \text{ km s}^{-1}$ ) and a starburst component ( $\lesssim 200 \text{ km s}^{-1}$ ). The density, ionisation parameter, number and total mass of Seyfert II narrow

line clouds all resemble local Seyferts, and our interpretation of the resonant scattering agrees with that of Villar-Martin et al. (1996) for high-redshift radiogalaxies. The flux from the narrowest  $H\alpha$  component is in excellent agreement with radiative transfer models which comprise similar quasar and starburst bolometric contributions.

## ACKNOWLEDGEMENTS

We thank Carlos Martin for assisting the observations. The WHT is operated on the island of La Palma by the Royal Greenwich Observatory in the Spanish Observatorio del Roque de los Muchachos of the Instituto de Astrofísica de Canarias. We thank Steve Eales for performing the GASP astrometry of the F10214 + 4724 field, and for (unwittingly) contributing observing time to the project. We also thank Tony Lynas-Gray, Geoff Smith and Steve Warren for useful discussions.

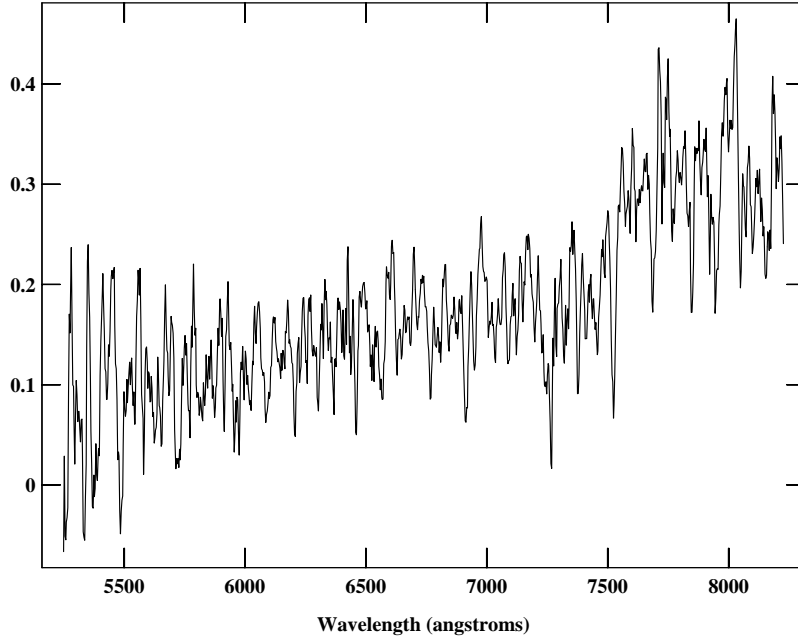
## REFERENCES

- Adams, T., 1972, MNRAS 174, 439  
 Barvainis R., Tacconi L., Antonucci R., Allion D., Coleman P., 1994, Nat, 371, 586  
 Bechtold, J., 1994, ApJ Suppl., 91, 1  
 Blandford, R.D., Kochanek, C.S., 1987, ApJ, 321, 658  
 Bland-Hawthorn, J., Sokolowski, J., Cecil, G., ApJ 375, 78  
 Broadhurst T. & Lehar J., 1995, ApJ Lett, 450, 41  
 Carico, D.P., Sanders, D.B., Soifer, B.T., Matthews, K., Neugebauer, G., 1988, ApJ, 100, 70  
 Charlot, S., Fall, S.M., 1991, ApJ 378, 471  
 Clements, D., van der Werf, P., Krabbe, A., Blietz, M., Genzel, R., Ward, M., 1993, Mon. Not. R. astr. Soc., 262, 23P  
 Condon, J.J., Anderson, M.L., Helou, G., 1991, ApJ, 376, 95  
 Condon, J.J., Huang, Z.-P., Yin, Q.F., Thuan, T.X., 1991, ApJ, 378, 65  
 Davidson, K., Netzer, H., 1979, Rev. Mod. Phys., 51, 715  
 De Robertis, M.M., Shaw, R.A., 1988, ApJ, 329, 629  
 Diaz, A.I., Prieto, M.A., Wamsteker, W., 1988, A & A, 195, 53  
 Downes, D., Radford, S.J.E., Greve, A., Thum, C., Solomon, P.M., Wink, J.E., 1992, ApJ, 398, L25  
 Downes, D., Solomon, P.M., Radford, S.J.E., 1995, ApJ, 453, 65  
 Dunlop, J.S., Hughes, D.H., Rawlings, S., Eales, S.A., Ward, M.J., 1994, Nat, 370, 347  
 Eisenhardt, P.R., Armus, L., Hogg, D.W., Soifer, B.T., Neugebauer, G., Werner, M.W., 1996, ApJ, 461, 72  
 Elston, R., McCarthy, P.J., Eisenhardt, P., Dickinson, M., Spinrad, H., Januzzi, B.T., Maloney, P., 1994, AJ, 107, 910  
 Ferland, G.J., 1993, University of Kentucky Department of Physics and Astronomy Internal Report  
 Ferland, G.J., 1996, *Hazy, a Brief Introduction to Cloudy*, University of Kentucky Department of Physics and Astronomy Internal Report

- Francis, P., Hewett, P., Foltz, C., Chaffee, F., Weymann, R., Morris, S., 1991, *ApJ*, 373, 465
- Giallongo, E., Cristiani, S., D'Odorico, S., Fontana, A., Savaglio, S., 1996, *ApJ* 466,46
- Goodrich, R., Miller, J., Martel, A., Cohen, M., Tran, H., 1996, *ApJ*, 456, L9
- Graham, J.R. & Liu, M.C., 1995, *ApJ*, in press
- Green, S.M., Rowan-Robinson, M., 1996, *MNRAS* 279, 884
- Haehnelt, M.G., Steinmetz, M., Rauch, M., 1997, preprint, submitted to *ApJ*
- Hines, D.C., Schmidt, G.D., Cutri, R.M., Low, F.J., 1995, *ApJ Lett*, 450, 1
- Iwamuro, F., Maihara, T., Tsukamoto, H., Oya, S., Hall, D.B., Cowie, L.L., 1995, *PASJ*, 47, 265
- Jannuzi, B.T., Elston, R., Schmidt, G.D., Smith, P.S., Stockman, H.S., 1994, *ApJ*, 429, L49
- Kennicutt, R.C., Jr., 1983, *ApJ*, 272, 54
- Kennicutt, R.C., Jr., Tamblyn, P., Congdon, C.E., 1995, *ApJ* 435, 22
- Kriss, G.A., *et al.*, 1992a, *ApJ*, 392, 485
- Kriss, G.A., *et al.*, 1992b, *ApJ Lett*, 394, 37
- Kroker, H., Genzel, R., Krabbe, A., Tacconi-Garman, L.E., Tecza, M., Thatte, N., 1996, *ApJL*, 463, 55
- Langston G.I., Conner S.R., Lehár J., Burke B.F., Weiler K.W., *Nat*, 1990, 344, 43
- Larkin J.E., *et al.*, 1994, *ApJ*, 420, L9
- Lawrence, A., Rowan-Robinson, M., Oliver, S., Taylor, A., McMahon, R.G., Broadhurst, T., Scarrot, S.M., Rolph, C.D., Draper, P.W., Ellis, R.S., Tadhunter, C., Condon, J.J., Lonsdale, C.J., Hacking, P., Conrow, T., Efsthathiou, G.P., Saunders, W.S., 1993, *MNRAS*, 260, 268
- Leech, K.J., Penston, M.V., Terlevich, R., Lawrence, A., Rowan-Robinson, M., Crawford, C., 1989, *MNRAS* 240, 349
- Matthews K., *et al.*, 1994, *ApJ*, 420, L13
- Moorwood, A.F.M., 1996, *Space Science Reviews*. 77, 303
- Mountain, C.M., Robertson, D.J., Lee, T.J., Wade, R., 1990, *Instrumentation in Astronomy VII*, ed. D.L. Crawford (Proc. SPIE, 1235), 25
- Narayan R., Wallington S., 1992, in Kayser R., Schramm T., Nieser L., eds, *Gravitational Lenses*. Springer-Verlag, Berlin, p. 12
- Nadeau, D., Yee, H.K.C., Forrest, W.J., Garnett, J.D., Ninkov, Z., Pipher, J., 1991, *ApJ*, 376, 430
- Nelson, C.H., Whittle, M., 1996, *ApJ*, 465, 96
- Neufeld, D.A., McKee, C.F., 1988, *ApJ*, 331, L87
- Osterbrock, D.E., 1989, *Astrophysics of Gaseous Nebulae and Active Galactic Nuclei*, University Science Publications, Mill Valley, CA, USA
- Osterbrock, D.E., 1993, *ApJ* 404, 551
- Pei, Y., 1992, *ApJ* 395, 130
- Phinney, E.S., 1989, *Theory of Accretion Disks*, W. Dush, F. Meyer and J. Frank, eds, (Dordrecht: Kluwer Academic Publishers) pp 457-470
- Radford, S.J.E., Brown, R.L., Vanden Bout, P.A., 1993, *A & A*, 271, L21
- Ramsay, S.K., Mountain, C.M., Geballe, T.R., 1992, *MNRAS*, 259, 751
- Rocca-Volmerange B., Guiderdoni B., 1988, *A&AS* 75, 93
- Rowan-Robinson, M., 1995, *MNRAS*, 272, 737
- Rowan-Robinson, M., Crawford, C., 1989, *MNRAS*, 238, 523
- Rowan-Robinson, M., *et al.*, 1991, *Nat*, 351, 719
- Rowan-Robinson, M., *et al.*, 1993, *MNRAS*, 261, 513
- Scoville, N.Z., Yun, M.S., Brown, R.L., Vanden Bout, P.A., 1995, *ApJ*, 449, L109
- Serjeant, S., Lacy, M., Rawlings, S., King, L.J., Clements, D.L., 1995, *MNRAS* 276, L31
- Snidjers, M.A.J., Netzer, H., Boksenberg, A., 1986, *MNRAS*, 222, 549
- Soifer, B.T., Cohen, L., Armus, K., Matthews G., Neugebauer G., Oke J.B., 1995, *ApJ*, 443, L65
- Soifer, B.T., Neugebauer, G., Matthews, K., Lawrence, C., and Mazzarella, J., 1992, *ApJ*, 399, L55
- Solomon, P.M., Downes, D., Radford, S.J.E., 1992, *ApJ*, 398, L29
- Sopp, H.M., Alexander, P., 1991, *MNRAS*, 251, 14P
- Steidel, C.C., Giavalisco, M., Pettini, M., Dickinson, M., Adelberger, K.L., 1996, *ApJ Lett*, 462, 17
- Thronson, H.A., Majewski, S., Descartes, L., Hereld, M., 1990, *ApJ* 364, 456
- Tran, H., 1995, *ApJ*, 440, 597
- Trentham, N., 1995, *MNRAS*, 277, 616
- Turner E.L., Ostriker J.P., Gott J.R., 1984, *ApJ*, 284, 1
- Villar-Martin, M., Binette, L., Fosbury, R.A.E., 1996, *A & A* 312, 751
- Wolfe, A.M., Lanzetta, K.M., Foltz, C.B., Chaffee, F.H., 1995, *ApJ* 454, 698
- Warren, S., Hewett, P., Osmer, P., 1994, *ApJ*, 421, 412
- Wilson, C.D., Walker, C.E., Thornley, M.D., 1997, *ApJ* 482, 131

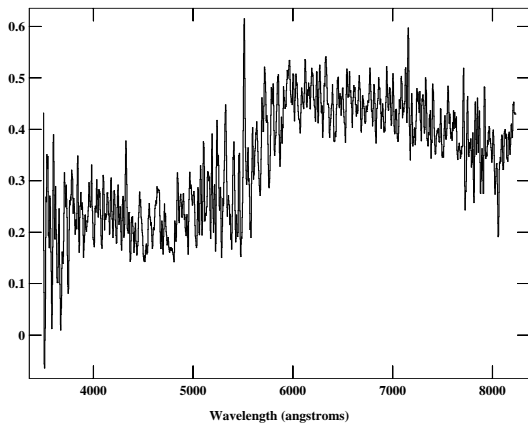
## 7 APPENDIX A: COMPANION GALAXIES

Figure A1 shows the spectrum of a galaxy  $\sim 19''$  south-west of the IRAS galaxy, which fortuitously lay on the slit in our WHT observations. The feature at around  $5510\text{\AA}$  is a probably a low energy cosmic ray event, but the emission lines at  $7155\text{\AA}$  and (marginally) at  $5323\text{\AA}$  appear to be real, since they occur in the spectra at both nights. Cross-correlating this spectrum with old galaxy models (a 1-Gyr burst aged by  $6 \times 10^8$  years to 1 Gyr) from Bruzual & Charlot (1993) yields two redshift estimates, 0.428 and 0.476 (both  $\pm \sim 5\%$ ) We prefer the former, which identifies the weak emission features as [OII]3727 and [OIII]5007. Close *et al.* (1995) report a similar redshift,  $0.429 \pm 0.002$  for a further galaxy  $\sim 23''$  south-west of the IRAS galaxy. The UV upturn in figure A1 may indicate a recent starburst, as expected perhaps if the galaxies are tidally interacting. However, there could be a slight systematic error in the redshift of the Close *et al.* companion. The emission line wavelengths in their spectrum of F10214+4724 are offset by a factor  $\sim 0.99$  compared to other published spectra (*e.g.* Goodrich *et al.* 1995, Rowan-Robinson *et al.*



**Figure A2.** The sum of the spectra of sources 2 and 3 (in the notation of Matthews *et al.* 1994). These spectra were extracted with 3 pixel ( $\sim 1.1''$ ) apertures, differing slightly to the method of Serjeant *et al.* 1995, though with very little quantitative difference. Source 2 is corrected for contamination by the IRAS galaxy by subtracting a spectrum of F10214+4724 scaled by the strength of the CIII]1909 line. The sum has been smoothed with a 5-pixel ( $\sim 14\text{\AA}$ ) boxcar. The flux has units  $10^{-20} \text{ W m}^{-2} \text{ \AA}^{-1}$ .

1993), and the residuals from the  $5577\text{\AA}$  sky feature also appear to be offset by a similar amount.



**Figure A1.** Serendipitous galaxy  $\sim 19''$  south-west of F10214+4724. The flux has units  $10^{-20} \text{ W m}^{-2} \text{ \AA}^{-1}$ , and the spectrum is extracted with a full width zero intensity aperture.

*et al.* 1995) is consistent with both its velocity dispersion (*e.g.* Broadhurst & Léhar 1995) and surface brightness profile (Eisenhardt *et al.* 1996). Further support for this lens redshift comes from figure A2, in which the spectra of sources 2 and 3 (Serjeant *et al.* 1995) are summed. Source 2 is the lensing galaxy and source 3 is the companion  $\sim 3.3''$  north east of the IRAS galaxy, in the notation of Matthews *et al.* (1994). If the galaxies are indeed associated, as suggested by their similar spectral energy distributions and tentative  $4000\text{\AA}$  breaks (Serjeant *et al.* 1995), as well as hints of tidal interaction in HST imaging (Eisenhardt *et al.* 1995), then the summed spectrum should show a  $\sim \sqrt{2}$  improvement in signal-to-noise, which is indeed the case in figure A2.

Several groups have also noted the slight overdensity of galaxies in the vicinity of F10214+4724. The discovery of a MgII absorber in the Keck spectrum at  $z = 1.316$  (Goodrich *et al.* 1995), and the possibly associated pair at  $z \simeq 0.4$ , implies that several physically independent systems, at a variety of redshifts, contribute to the overdensity in the field.

## 8 APPENDIX B: THE MYSTERY LINE AT 2067Å

In this section we summarise our attempts to identify the line at 2067Å in the rest-frame spectrum of F10214+4724. We have made an extensive literature search, and investigated synthetic spectra generated by the CLOUDY photoionisation code over wide ranges of ionisation parameter and abundances (v84.12, Ferland 1995; and see section 4.2). This led to only two possible identifications for this line. The first of these is the resonant boron BIII 2068 doublet, the next resonance line in the Lithium isoelectronic sequence below the bright OVI, NV and CIV lines. The tiny cosmic abundance of boron means that this line is predicted to be immeasurably faint, and we therefore reject this possibility. The second possibility is the forbidden [NaV] 2067.9/2069.8 doublet (Mendoza 1983) - a line which is not found in the CLOUDY v84.12 output.

To determine whether the [NaV] 2067.9/2069.8 doublet is a plausible identification for the mystery line we have compared its predicted strength with that of [Ne IV] 2422.5/2425.1. These two pairs of collisionally-excited lines arise from electronic transitions within adjacent ions in the Nitrogen isoelectronic sequence. In the low-density limit the ratio of the cooling rates in these doublets is given by

$$\frac{L_{2069}}{L_{2424}} = \frac{n_{NaV}}{n_{NeIV}} \times \frac{e^{-\frac{\chi_{2069}}{kT}}}{e^{-\frac{\chi_{2424}}{kT}}} \times \frac{\Omega_{2069}}{\Omega_{2424}} \times \frac{2424}{2069} \quad (10)$$

(Osterbrock 1989), where  $\chi_{\lambda}$  is the excitation potential of the upper energy level(s) and  $\Omega_{\lambda}$  is the effective collision strength (see Mendoza 1983).

Adopting  $T = 10^4$  K and solar abundances, and assuming that the fraction of Na in the  $Na^{4+}$  state is similar to the fraction of Ne in the  $Ne^{3+}$  state, the value of this ratio is  $\approx 0.005$ . The measured ratio is  $\approx 0.23$  so at first sight the putative [NaV] 2067.9/2069.8 doublet would need to be anomalously strong. However, at higher densities, collisional de-excitation may become important. The critical densities for collisional de-excitation  $n_{crit}$  are  $\sim 10^{11} \text{ m}^{-3}$  and  $\sim 10^{12} \text{ m}^{-3}$  for the lower wavelength lines in the Ne and Na doublets respectively (in each case the higher wavelength doublet line has an order of magnitude lower  $n_{crit}$  than its partner). Given the weakness of the [OII]3727 line, with  $n_{crit} \sim 10^{10} \text{ m}^{-3}$ , in F10214+4724, and the strengths of the [OIII]4959/5007 line and forbidden neon lines (with  $n_{crit} \gtrsim 10^{12} \text{ m}^{-3}$ ) (Soifer et al. 1995) it is certainly feasible that collisional de-excitation can account for the strength of the putative [NaV] doublet with respect to the [NeIV] doublet.

We conclude that the [NaV]2067.9/2069.8 doublet is a probable identification for the mystery line in the spectrum of F10214+4724, and, by analogy, in NGC1068 and other active galaxies.